

Electronic structure of black SmS. II. Angle-resolved photoemission spectroscopy

T. Ito

Department of Physics, Tohoku University, Sendai 980-8578, Japan

A. Chainani

*Institute for Plasma Research, Gandhinagar 382 428, India
and Department of Physics, Tohoku University, Sendai 980-8578, Japan*

H. Kumigashira and T. Takahashi

Department of Physics, Tohoku University, Sendai 980-8578, Japan

N. K. Sato

Department of Physics, Nagoya University, Chikusa-ku, Nagoya 602-4648, Japan

(Received 15 April 2001; published 26 March 2002)

We have studied the electronic band structure of semiconducting black SmS with high-resolution angle-resolved photoemission spectroscopy (ARPES). The valence band consists of two well-separated groups of bands: almost nondispersive bands near E_F and highly dispersive bands at higher binding energy. The former is ascribed to the Sm^{2+} ($4f^6 \rightarrow 4f^5$) multiplet and the latter to mainly the S $3p$ states. We found a small but distinct energy dispersion in the Sm $4f$ -derived bands near E_F . This indicates a strong hybridization between the “localized” Sm $4f$ electrons and the “itinerant” conduction electrons, leading to the “delocalized” Sm $4f$ states in mixed-valent SmS. We have compared the present ARPES results with a recent periodic Anderson model calculation [C. Lehner *et al.*, Phys. Rev. B **58**, 6807 (1998)].

DOI: 10.1103/PhysRevB.65.155202

PACS number(s): 71.28.+d, 75.30.Mb, 79.60.Bm

I. INTRODUCTION

Rare-earth compounds have attracted much attention because of their anomalous properties such as the mixed valence and Kondo effect.^{1–5} The interplay between the “localized” f electrons and the “itinerant” conduction electrons is regarded to play a crucial role in realizing such anomalous properties. In mixed-valent rare-earth compounds, where the interaction (hybridization) between f and conduction electrons is substantially strong, the f electrons acquire a delocalized character through the interaction and become to show an energy dispersion in momentum space. The resultant complicated energy-vs-momentum relation of f electrons is expected to produce a variety of anomalous properties. Angle-resolved photoemission spectroscopy (ARPES) is a unique experimental technique to directly study the electronic structure of solids as a function of momentum and has been applied to a variety of materials such as high- T_c cuprates and charge-density-wave compounds. While angle-integrated studies have been reliably used to study the electronic structure of Kondo systems for nearly 20 years,^{6,7} ARPES studies have been carried out only over the last few years^{8–10} because of several limiting factors such as the very small energy dispersion and the strong surface reactivity of samples. However, a recent remarkable improvement in the energy resolution and intensity enables ARPES study to unravel the experimental band structure of rare-earth compounds.^{8–10}

In the present work, we study the “band structure” of semiconducting black SmS, which is well known for the pressure-induced first-order transition to a golden mixed-valent phase.^{1,11,12} As discussed in the preceding paper, the electronic structure of SmS is being readdressed with im-

proved techniques of photoemission spectroscopy. Here we use ARPES to study the electronic structure and compare the experimentally determined band structure with a recent band structure calculation based on the periodic Anderson model using the local density approximation.¹³ The present ARPES results have elucidated a small but distinct energy dispersion of the $4f$ -derived states originating in the Sm^{2+} multiplet as well as highly dispersive S $3p$ bands, in qualitatively good agreement with the calculation. The observed energy dispersion in the $4f$ -derived bands suggests that the f -electron states strongly hybridize with the conduction electrons.

II. EXPERIMENT

Single crystals of SmS were obtained from the same batch used for the angle-integrated photoemission measurements in the preceding paper. The structure, electrical, and magnetic properties have been reported¹⁴ and match well with previous works.^{11,12} Photoemission measurements were carried out using a homebuilt high-resolution angle-resolved photoemission spectrometer based on a VSW HAC300 analyzer. The energy resolution was set at 100 and 200 meV for He I and He II measurements, respectively. The base pressure was 1×10^{-11} Torr and the angular resolution was $\pm 1^\circ$ and $\pm 3^\circ$ for He I and He II photons, respectively. A clean mirrorlike surface of SmS (001) plane was obtained by *in situ* cleaving at 30 K just before the measurement. The crystal orientation was determined roughly by the Laue diffraction before being transferred into the spectrometer and then precisely by the ARPES spectra measured around the high-symmetry point. Since we observed a relatively fast degradation of the crystal surface as seen from the gradual

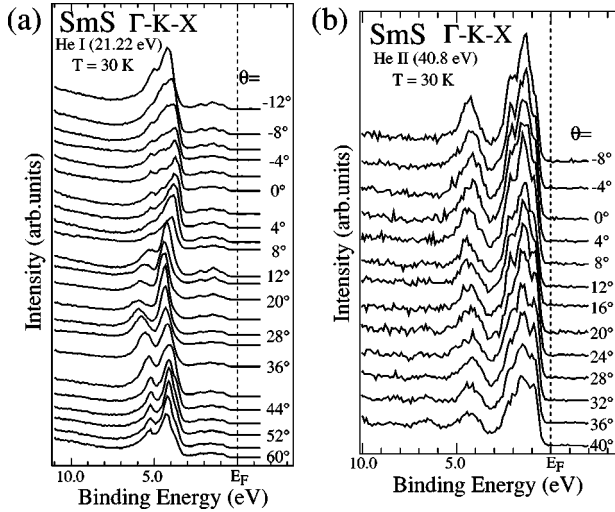


FIG. 1. High-resolution ARPES spectra of semiconducting black SmS measured at 30 K along ΓKX direction in the fcc Brillouin zone with (a) He I and (b) He II photons. The polar angle (θ) referred to the surface normal is indicated on each spectrum.

decrease of the intensity of a surface-originated peak as well as the increase of the background in the spectra, we recorded all the spectra before the degradation was evident (within 8 h after cleaving). The Fermi level (E_F) of sample was referenced to a gold film evaporated on the sample substrate.

III. RESULTS AND DISCUSSION

Figure 1 shows the ARPES spectra of semiconducting black SmS measured along the ΓKX direction in the fcc Brillouin zone (BZ) (Fig. 2) at 30 K with (a) He I (21.2 eV) and (b) He II (40.8 eV) photons. The spectra yield the momentum-resolved electronic structure in the $\Gamma KX-XK\Gamma$ plane (shaded area in Fig. 2) with a dominant contribution from the high-symmetry line of ΓKX . The polar angle (θ) referred to the surface normal of the cleaved plane is shown on each spectrum. The ARPES spectra exhibit several dispersive peaks over the whole valence-band region up to a bind-

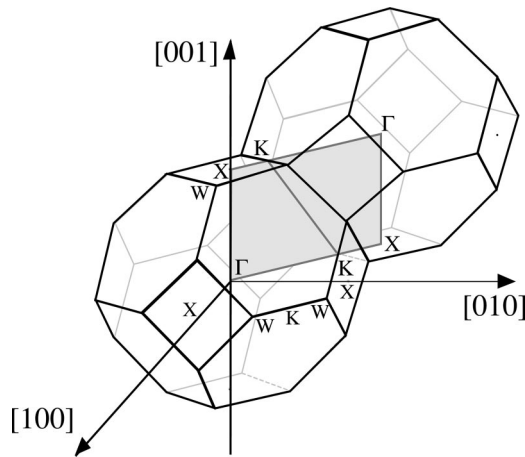


FIG. 2. Brillouin zone of fcc SmS in the extended zone scheme. Shaded area shows the $\Gamma KX-XK\Gamma$ plane.

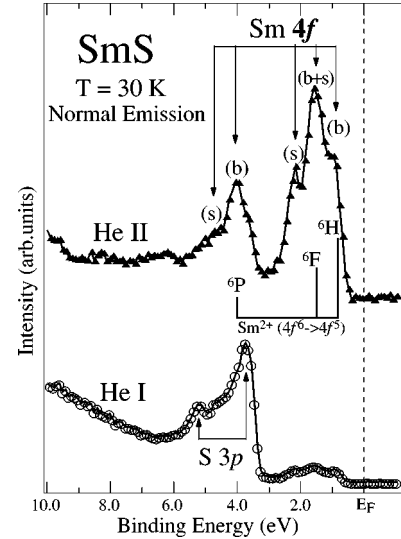


FIG. 3. Normal-emission ARPES spectra of SmS measured with He I (lower panel) and He II (upper panel) photons. The orbital character (Sm $4f$ or S $3p$) is shown on each peak, together with identification of the bulk (b) or surface (s) contribution. The multiplet structure due to the Sm^{2+} ($4f^6 \rightarrow 4f^5$) atomic level is shown on the He II spectrum.

ing energy of 6 eV, which consists of two groups of peaks: one is located between 3.5 and 6 eV binding energy and another being at $E_F - 2.5$ eV. The two groups of peaks are clearly distinguished by the considerably different relative intensities between He I and He II photons. The He I spectra show remarkable and systematic dispersive features at 3.5–6 eV as a function of θ , while the peaks at $E_F - 2.5$ eV look almost dispersionless. In order to see the photon energy dependence more clearly, we compare normal-emission ARPES spectra measured with He I and He II photons in Fig. 3. Since the photoionization cross section of the S $3p$ states decreases with increasing photon energy while that of the Sm $4f$ states increases,¹⁵ peaks near E_F are assigned to the Sm $4f$ states while the highly dispersive features at higher binding energy are to mainly the S $3p$ states. This assignment is consistent with early ultraviolet photoemission spectroscopy (UPS) studies^{16–19} as well as the results discussed in the preceding paper.

It has been reported that the three-peaked structure at $E_F - 2.5$ eV in the UPS spectrum transforms into a two-peaked structure in the x-ray photoemission spectrum (XPS).¹⁸ A similar spectral variation has been also observed in the UPS spectrum itself upon oxygen exposure.¹⁹ These experimental results suggest that the He II spectrum is composed of both the bulk and surface components well described with the multiplet structure of the Sm^{2+} ($4f^6 \rightarrow 4f^5$) atomic level as shown in Fig. 3. The energy separation between the two components is about 0.6 eV. We find in Fig. 3 that the bulk 6P feature overlaps the broad S $3p$ states at 3.5–6 eV and shows a slight angular dependence as observed in Fig. 1(b). This suggests a substantial hybridization between the Sm $4f$ and S $3p$ states in this energy region.

In order to see the dispersive feature of bands more clearly, we have mapped out the “band structure” and show

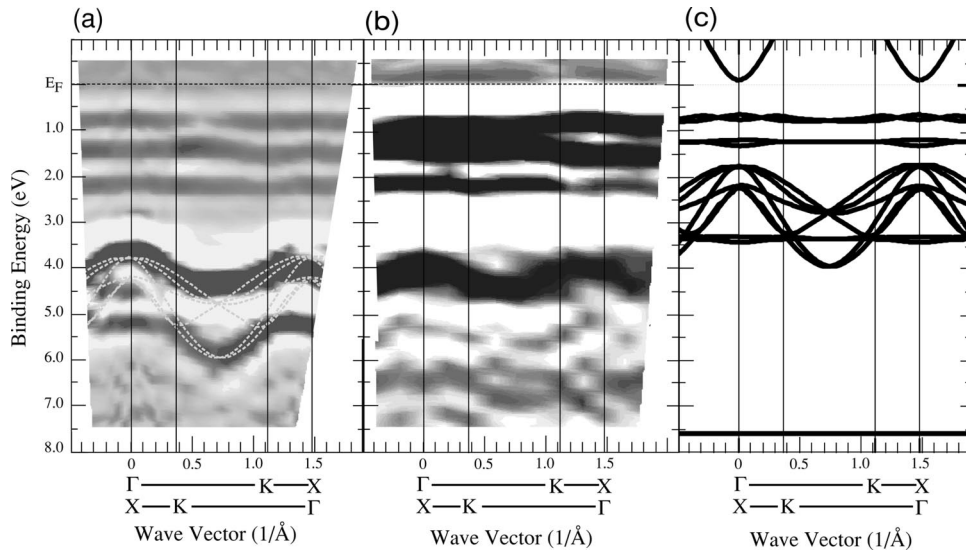


FIG. 4. Experimental band structure of semiconducting black SmS determined by ARPES using (a) He I and (b) He II photons, compared with (c) the band structure calculation based on the periodic Anderson model (Ref. 13). White dashed lines in (a) show the calculated S 3*p* bands shifted by 2 eV toward higher binding energy.

the results in Fig. 4. The experimental band structure was obtained by taking the second derivative of ARPES spectra after moderate smoothing and plotting the intensity as a function of the wave vector and the binding energy. The dark areas in Figs. 4(a) and 4(b) correspond to the “bands.” We set the gray scale so as to have the apparent bandwidth in the gray-scale image to be almost equal to the full width at half maximum of the corresponding peak in Fig. 1. This second-derivative method has been widely used in many materials, such as high-temperature superconductors,²⁰ heavy-fermion compounds,⁹ etc., to avoid artificial errors included in the case of picking up the peak position by eye. The correct peak position is often masked by the background due to the secondary electrons, which is removed by this method. In both band structures obtained by He I and He II photons [Figs. 4(a) and 4(b)], we find two well-separated groups of bands located at $E_F - 2.5$ eV and 3.5–6 eV, respectively, as expected from the ARPES spectra in Fig. 1. As discussed above, the three slightly dispersive bands at $E_F - 2.5$ eV are ascribed to the Sm 4*f* states while the highly dispersive bands at 3.5–6 eV are due to mainly the S 3*p* states.

Figure 4(c) shows the band structure of semiconducting black SmS calculated based on the periodic Anderson model¹³ (PAM) for comparison. The calculated bands are symmetrized with respect to the midpoint between Γ and X points to directly compare with the experimental band dispersions in Figs. 4(a) and 4(b). We at first notice that the gross feature of band dispersions shows a qualitatively good agreement between the experiment and calculation, except for a clear discrepancy of relative position of the Sm 4*f* and S 3*p* bands. The S 3*p* bands are located much closer to E_F in the calculation than the experiment. We found that a rigid shift of calculated S 3*p* bands by 2 eV toward high binding energy leads to a quantitatively good agreement, as shown in Fig. 4(a). The reason(s) for this discrepancy is unknown at present. The band structure calculation may have underestimated the S 3*p* atomic level itself and/or the hybridization strength between the S 3*p* and the Sm 4*f* states. In both cases, the S 3*p* bands are expected to be pulled down toward the high binding energy. A model band calculation, where the

lattice parameter is artificially varied to simulate the hybridization strength, shows that the S 3*p* band is shifted downward with increasing the hybridization.²¹ However, the calculated energy shift is smaller than the observed difference (2 eV) within a reasonable parameter range, suggesting that the observed discrepancy in the energy position of the S 3*p* band is not accounted for only by the hybridization, but is also attributed to the bare S 3*p* level in the calculation.

In the experimental band structure obtained by He II photons [Fig. 4(b)] where the Sm 4*f* states are relatively enhanced, we find three slightly dispersive bands near E_F . According to the discussion above (Fig. 3), the first band closest to E_F is assigned to one component (6H) of the multiplet structure of bulk Sm²⁺, the second one to an admixture of the surface 6H counterpart and the bulk 6F component, and the third one located around 2 eV to the surface 6F multiplet structure. So we can compare the first two experimental bands with the calculation. As shown in Fig. 4(c), the calculation predicts three almost nondispersive Sm 4*f* “bands” at 0.7, 1.3, and 3.3 eV. Although the deepest component at 3.3 eV may correspond to a broad experimental band located at 4 eV in the He II band structure, it is apparently overlapped by the S 3*p* bands so that the dispersive feature is not clearly resolved. In contrast, two Sm 4*f* bands closer to E_F are well separated from the S 3*p* bands. We find by comparison that the experimental Sm 4*f* bands are located at a slightly higher binding energy than the calculated bands, and what is more important is that the experimental bands are more dispersive than the calculated ones. One may infer that the surface sensitivity as a function of angle in ARPES measurements produces the apparent energy dispersion since the bulk and the surface band are located very close to each other. However, as shown in Fig. 1, the relative intensity of the surface peak at 2 eV to the bulk peak at 1 eV *decreases* on moving from the $\Gamma(X)$ to the $X(\Gamma)$ point whereas the surface sensitivity increases. Furthermore, as shown in Fig. 4, the band dispersion near E_F is not monotonic as a function of angle (momentum). All these indicate that the observed dispersive feature is intrinsic and is not due to the simple angle-dependent

surface sensitivity in ARPES measurements. It is also noted that the energy separation between the two Sm $4f$ bands is larger in the experiment than in the calculation around the $X(\Gamma)$ point where a substantial admixture of Sm $5d$ states is predicted from the band calculation.^{13,21} All these facts unambiguously indicate that the Sm $4f$ states form dispersive “bands” through hybridization with conduction electrons, although the corresponding peaks in the ARPES spectrum are qualitatively well understood in terms of the atomic multiplet structure of Sm^{2+} . The present ARPES results thus indicate that the hybridization between the “localized” Sm $4f$ electrons and “itinerant” conduction electrons plays a crucial role in characterizing the semiconducting mixed-valent black SmS.

IV. CONCLUSIONS

We have performed high-resolution angle-resolved photoemission spectroscopy on semiconducting black SmS and experimentally determined the “band structure.” The va-

lence band consists of two well-separated groups of bands: almost nondispersive bands at $E_F - 2.5$ eV and highly dispersive bands at 3.5–6 eV. The former is ascribed to the Sm^{2+} ($4f^6 \rightarrow 4f^5$) multiplet structure while the latter to mainly the S $3p$ states. We clearly observed a small but distinct energy dispersion in the Sm $4f$ “bands.” This indicates the importance of the hybridization between the “localized” Sm $4f$ electrons and the “itinerant” conduction electrons in realizing the “delocalized” Sm $4f$ electrons and the resultant mixed-valent state of semiconducting black SmS. We have compared the present ARPES results with a recent periodic Anderson model calculation¹³ and found discrepancies in the energy position of the S $3p$ bands and the energy dispersion of the Sm $4f$ bands, although the gross feature of the band structure shows good qualitative agreement between the experiment and calculation.

This work was supported by a grant from MEXT of Japan. T.I. thanks the Japan Society for the Promotion of Science for financial support.

-
- ¹C. M. Varma, *Rev. Mod. Phys.* **48**, 219 (1976).
²O. Gunnarsson and K. Schönhammer, in *Handbook on the Physics and Chemistry of Rare Earths*, edited by K. A. Gschneidner, Jr., L. Eyring, and S. Hüfner (North-Holland, Amsterdam, 1987), Vol. 10, p. 103.
³G. R. Stewart, *Rev. Mod. Phys.* **56**, 755 (1984); A. C. Hewson, *The Kondo Problem to Heavy Fermions* (Cambridge University Press, Cambridge, England, 1993).
⁴L. Degiorgi, *Rev. Mod. Phys.* **71**, 687 (1999).
⁵P. Strange, A. Svane, W. M. Temmerman, Z. Szotek, and H. Winter, *Nature* (London) **399**, 756 (1999).
⁶J. W. Allen, S.-J. Oh, I. Landau, J. M. Lawrence, L. I. Johansson, and S. B. Hagström, *Phys. Rev. Lett.* **46**, 1100 (1981).
⁷M. Croft, J. H. Weaver, D. J. Peterman, and A. Franciosi, *Phys. Rev. Lett.* **46**, 1104 (1981).
⁸A. B. Andrews, J. J. Joyce, A. J. Arko, J. D. Thompson, J. Tang, J. M. Lawrence, and J. C. Hemminger, *Phys. Rev. B* **51**, R3277 (1995); A. B. Andrews, J. J. Joyce, A. J. Arko, Z. Fisk, and P. S. Riseborough, *ibid.* **53**, 3317 (1996).
⁹H. Kumigashira, S.-H. Yang, T. Yokoya, A. Chainani, T. Takahashi, A. Uesawa, T. Suzuki, O. Sakai, and Y. Kaneta, *Phys. Rev. B* **54**, 9341 (1996); H. Kumigashira, S.-H. Yang, T. Yokoya, A. Chainani, T. Takahashi, A. Uesawa, and T. Suzuki, *ibid.* **55**, R3355 (1997); H. Kumigashira, H.-D. Kim, A. Ashihara, A. Chainani, T. Yokoya, T. Takahashi, A. Uesawa, and T. Suzuki, *ibid.* **56**, 13 654 (1997).
¹⁰J. D. Denlinger, G.-H. Gweon, J. W. Allen, C. G. Olson, Y. Dalichaouch, B.-W. Lee, M. B. Maple, Z. Fisk, P. C. Canfield, and P. E. Armstrong, *Physica B* **281&282**, 716 (2000).
¹¹A. Jayaraman, V. Narayannamurti, E. Bucher, and R. G. Maines, *Phys. Rev. Lett.* **25**, 1430 (1970); A. Jayaraman, A. K. Singh, A. Chatterjee, and S. Usha Devi, *Phys. Rev. B* **9**, 2513 (1974); A. Jayaraman, P. Dernier, and L. D. Longinotti, *ibid.* **11**, 2783 (1975).
¹²S. D. Bader, N. E. Phillips, and D. B. McWhan, *Phys. Rev. B* **7**, 4686 (1973).
¹³C. Lehner, M. Richter, and H. Eschrig, *Phys. Rev. B* **58**, 6807 (1998).
¹⁴M. Ohashi, D. Kondo, N. Sato, T. Suzuki, T. Komatsubara, H. Takahashi, and N. Môri, *Rev. High Pressure Sci. Technol.* **7**, 611 (1998).
¹⁵J. J. Yeh and I. Lindau, *At. Data Nucl. Data Tables* **32**, 1 (1985).
¹⁶J. L. Freeouf, D. E. Eastman, W. D. Grobman, F. Holtzberg, and J. B. Torrance, *Phys. Rev. Lett.* **33**, 161 (1974).
¹⁷G. Krill, J. P. Senateur, and A. Amamou, *J. Phys. F: Met. Phys.* **10**, 1889 (1980).
¹⁸W. Gudat, M. Campagna, R. Rosei, J. H. Weaver, W. Eberhardt, F. Hulliger, and E. Kaldis, *J. Appl. Phys.* **52**, 2123 (1981).
¹⁹N. Martensson, B. Reihl, R. A. Pollak, F. Holtzberg, and G. Kaindl, *Phys. Rev. B* **25**, 6522 (1982).
²⁰D. H. Lu, D. L. Feng, N. P. Armitage, K. M. Shen, A. Damascelli, C. Kim, F. Ronning, Z.-X. Shen, D. A. Bonn, R. Liang, W. N. Hardy, A. I. Rykov, and S. Tajima, *Phys. Rev. Lett.* **86**, 4370 (2001); A. Ino, C. Kim, M. Nakamura, T. Yoshida, T. Mizokawa, Z.-X. Shen, A. Fujimori, T. Kakeshita, H. Eisaki, and S. Uchida, *Phys. Rev. B* **62**, 4137 (2000).
²¹P. Strange, *J. Phys. C* **17**, 4273 (1984).